Hydration Structure and Water Exchange Reaction of Nickel(II) Ion: Classical and QM/MM Simulations

Yasuhiro Inada,*,† Ahmed M. Mohammed,‡ Hannes H. Loeffler, and Bernd M. Rode

Department of Theoretical Chemistry, Institute for General, Inorganic and Theoretical Chemistry, University of Innsbruck, A-6020 Innsbruck, Austria

Received: August 30, 2001; In Final Form: March 22, 2002

Classical molecular dynamics (MD), classical Monte Carlo (MC), and combined quantum mechanical/molecular mechanical (QM/MM) MD simulations were carried out to investigate the hydration structure of the Ni(II) ion in water using a newly constructed 2-body potential and a function correcting for 3-body effects. A 6-coordinate hydration structure with a maximum probability of the Ni−O distance at 2.25, 2.21, and 2.14 Å was observed by the classical MD, classical MC, and QM/MM-MD simulation with 3-body corrections, respectively, while an 8-coordinate structure was observed by the classical MD and MC simulations using only 2-body pair potentials. The average structure parameters obtained by the Hertree-Fock level QM/MM-MD simulation are in agreement with the experimental values. The validity of the 3-body correction function is discussed on the basis of the results for the classical and QM/MM simulations. During the classical MD simulation, a water exchange reaction was observed for the 6-coordinate Ni(II) ion. The water exchange reaction proceeded via a 5-coordinate intermediate with the lifetime of ca. 2.5 ps. The observed dissociative mechanism of the water exchange reaction is in accordance with experimental evidence.

Introduction

The hydration structure of the Ni(II) ion has been well investigated using various experimental methods.[1] The structural parameters, such as the coordination number and the Ni−O distance, have been determined in aqueous solutions as summarized in Table S1 (S: Supporting Information). The majority of those studies indicates that the Ni(II) ion is coordinated by six H_2O molecules in the first coordination sphere. Furthermore, the $[Ni(H_2O)_6]^{2+}$ fragment is observed in many single crystals, as summarized in Table S2. The octahedral arrangement of six H_2O molecules in the first coordination sphere is consistent with that observed in aqueous solutions. According to the compiled Ni−O distances for 37 samples in aqueous solutions and 38 samples in single crystals (see Tables S1 and S2, respectively), the maximum probability of the Ni−O distance is considered to be at ca. 2.06 Å, as shown in Figure S1. In marked contrast to the amount of experimental studies, not many molecular simulations on the Ni(II) ion have been reported,[2−5] although molecular dynamics (MD) and Monte Carlo (MC) simulations are very useful to obtain the molecular structure of hydrated ions such as Ni(II).[6,7]

In classical molecular simulation techniques, 2-body potential functions are used to describe the interactions between the metal ion and H_2O, and pairwise additivity of the 2-body contributions is assumed. The parameters of the 2-body potential function are generally determined in either an empirical or a theoretical way. In the former approach, partial atomic charges in the Coulombic term and potential parameters in a non-Coulombic term are empirically optimized so that the simulation reproduces structural, thermodynamic, and other macroscopic properties determined experimentally. Although such empirical pair potentials are very useful in molecular simulations, it is impossible to construct in the case of systems for which physicochemical quantities are experimentally not available. On the other hand, in the case of quantum theory-based 2-body potentials, the potential parameters are determined on the basis of pair interaction energies obtained by ab initio molecular orbital calculations. Such ab initio 2-body potentials have been constructed for a variety of metal ions interacting with water.[8−12]

However, ab initio molecular orbital calculations on $[M(H_2O)_n]^{m+}$ (M = metal) have clearly demonstrated that the stepwise binding of H_2O molecules leads to gradually decreasing binding energies.[13−19] This means that additivity of ab initio 2-body pair potentials cannot be assumed for $[M(H_2O)_n]^{m+}$. The reduced interaction energy between $[M(H_2O)_{n-1}]^{m+}$ and H_2O with increasing n is interpreted to be caused by both the neutralization of the positive charge on the metal ion and the exchange repulsion in the ion−H_2O interaction due to the existence of other H_2O molecules in the first coordination sphere.[20−25] A similar but opposite nonadditivity of ab initio 2-body potentials has been pointed out for H_2O molecules in the second hydration sphere;[21−26] i.e., the binding energy between the metal ion and H_2O is enhanced by the charge polarization due to the H_2O molecule in the second hydration sphere. These many-body contributions are quite important and their neglect leads to overestimations of the hydration number of the metal ion.[2,27−35]

Two main methods have been followed in an attempt to solve the many-body problem. One is the adoption of a polarizable or dissociative model for the H_2O molecule. Since such models can implicitly include many-body corrections, the experimental first-shell structure and energy of hydration are fairly well reproduced.[3,36−40] The other approach is to add 3-body correction functions to the ab initio 2-body potentials: the energy of

* To whom correspondence should be addressed. E-mail: yinada@lac.chem.nagoya-u.ac.jp.

† Permanent address: Research Center for Materials Science, Nagoya University, Chikusa, Nagoya 464-8602, Japan.

‡ Permanent address: Department of Chemistry, Addis Ababa University, P.O. Box 1176, Addis Ababa, Ethiopia.

10.1021/jp0155314 CCC: $22.00
Published on Web 06/28/2002

$[M(H_2O)_2]^{m+}$ cluster is computed by means of ab initio molecular orbital calculations and the nonadditive interaction energies for the 3-body assemblies are fitted to an analytical function. This approach can also reproduce the experimental hydration structure and energy of metal ions,[41−44] but the importance of higher-order corrections has been pointed out for transition metal ions.[45,46] Because there are many possible configurations of $[M(H_2O)_n]^{m+}$ ($n > 3$) to describe the energy surface for higher-order corrections, the total amount of necessary SCF-energy calculations becomes quickly unfeasible. Furthermore, it is nearly impossible to reproduce higher-order correction terms with a suitable analytical expression.

In principle, the many-body problem can be managed by quantum mechanical treatment of the whole solute/solvent system during the molecular simulation; i.e., energies and forces are calculated by solving the time-independent Schrödinger equation, and nuclear motions are evaluated according to the Born−Oppenheimer approximation. As this leads to unrealistic computational requirements, one can split the system into an inner, quantum mechanically treated region and an outer region, described by classical molecular mechanics.[47−52] With such combined quantum mechanical/molecular mechanical (QM/MM) methods, excellent agreement with experimental values was obtained for many physicochemical properties,[53−58] in particular for the solvation structure of metal ions.[59−67]

In the present study, the 2-body pair potential between Ni^{2+} and H_2O and its 3-body correction terms were evaluated by means of ab initio molecular orbital calculations, and corresponding analytical functions were constructed. With the 2-body potential and the 3-body correction function, classical MD and MC simulations were carried out. Furthermore, QM/MM-MD simulations were performed to investigate the hydration structure of the Ni(II) ion.

In addition to the hydration structure, ligand exchange and substitution reactions at the Ni(II) ion have been extensively studied using experimental techniques.[68−71] The ligand substitution has been a subject of numerous investigations because of the slow exchange reaction rate of hydrated Ni(II), in relation to other divalent transition metal ions. An interpretation of the reaction mechanism has been proposed since the early 1960s.[68−71] The measured rate constants have been traditionally analyzed on the basis of the so-called Eigen-Wilkins mechanism,[72] in which the ligand substitution reaction is considered to be composed of a fast preequilibrium step to form an "outer-sphere encounter" and a rate-determining binding change between a coordinated H_2O molecule and the first donating atom of an entering ligand. The equilibrium constant (K_{OS}) of the preassociation is generally estimated by using the electrostatic model based on the extended Debye−Hückel theory.[73] The measured second-order rate constant is then divided by K_{OS} to estimate the first-order rate constant (k_{ex}) for the rate-determining ligand exchange between a first shell water and the outer sphere ligand. It was pointed out that the k_{ex} value of the Ni(II) ion is almost independent of the donating ability of the entering ligand.[68−71] The spontaneous dissociation of the bound H_2O molecule from the Ni(II) ion is thus interpreted as the rate-determining step of ligand substitution reactions, i.e., a "dissociative" mechanism according to the classification by Langford and Gray.[74] Merbach et al. have determined the rate constant of the most basic water exchange reaction at the Ni(II) ion and found that the activation volume ($\Delta^{\ddagger}V°$) is positive ($+7.2$ cm^3 mol^{-1}) by using a high-pressure ^{17}O NMR technique.[75] Since the dissociation of an H_2O molecule from the first coordination sphere is considered to lead to an increase in partial molar volume of the system, the positive $\Delta^{\ddagger}V°$ value is claimed to be in accordance with the interpretation of the dissociative mode of activation. The dissociative mechanism and the positive $\Delta^{\ddagger}V°$ value have been supported by ab initio molecular orbital calculations on $[Ni(H_2O)_n]^{2+}$ ($n = 5-7$) performed by Rotzinger.[76,77] Tsutsui et al. have also reported the results of frequency analysis on $[Ni(H_2O)_7]^{2+}$ to reject the existence of the alternative associative and interchange paths during the water exchange reaction.[78] However, to date, no MD study describing the ligand exchange reaction at Ni(II) ion has been reported, although some MD simulations have been carried out to evaluate the water exchange mechanism for alkali metal(I)[79−81] and lanthanide(III) ions.[40] In this paper, the trajectories of dissociating and entering H_2O molecules for the water exchange reaction at the Ni(II) ion will be presented for the first time, and the ligand motions around the Ni(II) ion during the water exchange process will be discussed.

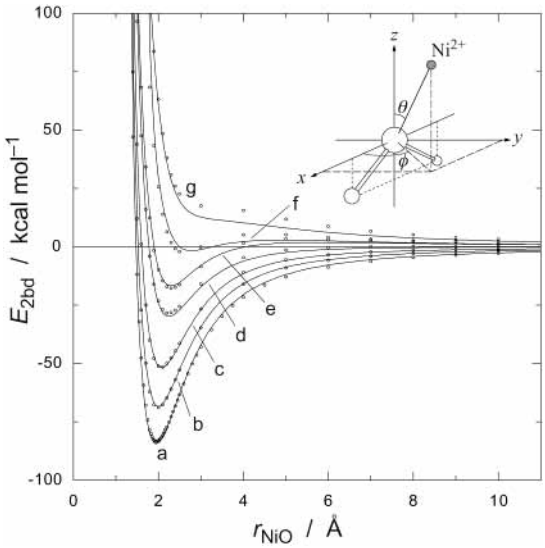

Figure 1. 2-Body pair potential between Ni(II) ion and H_2O. The SCF-calculated energies and fitted functions are shown by dotted and solid lines, respectively, at (θ, ϕ) = (0°, 0°) (a), (50°, 50°) (b), (70°, 50°) (c), (90°, 50°) (d), (120°, 90°) (e), (120°, 50°) (f), and (180°, 0°) (g). The definition of angles, θ and ϕ, is schematically depicted in the inset.

Details of Calculations

Evaluation of the 2-Body Potential Function. Ab initio molecular orbital calculations were carried out at the unrestricted Hartree−Fock (UHF) level using the Gaussian98 program.[82] The Los Alamos effective core potential (ECP) plus valence double-ζ (DZ) basis set[83] for Ni^{2+} and the valence DZ basis set[84] for H_2O with polarization function on the O atom were employed. The experimental gas-phase geometry of H_2O was fixed with the O−H distance of 0.9601 Å and the H−O−H angle of 104.47°.[85]

To calculate 2-body interaction energies between Ni^{2+} and H_2O, the position of the Ni^{2+} ion was varied around the H_2O molecule by fixing the O atom at the origin, two H atoms on the *xz* plane, and the C_{2v} axis of H_2O on the *z* axis of the Cartesian coordinate system (see the inset in Figure 1). The values of the Ni−O distance (r_{NiO}), the angle between the O−Ni vector and the *z* axis (θ), and the angle between the *x* axis and the projection of the O−Ni vector onto the *xy* plane (ϕ) were varied over the ranges 1.2 Å $\le r_{NiO} \le$ 10.0 Å, 0° $\le \theta \le$ 180°, and 0° $\le \phi \le$ 90°. SCF energy calculations were carried out for about 4300 configurations to cover the whole configuration space. The 2-body interaction energies (E_{2bd}) were calculated

TABLE 1: Optimized Potential Parameters for 2-Body Pair Potential and 3-Body Correction Function between Ni(II) Ion and H_2O

parameter	value	unit
	2-Body Potential Parameters	
Q_{Ni}	2.0000[a]	au
Q_O	−0.6596[a]	au
Q_H	0.3298[a]	au
A_O	−7577.8511834	kcal mol^{-1} Å^5
B_O	42716.9882874	kcal mol^{-1} Å^7
C_O	−70268.4505341	kcal mol^{-1} Å^9
D_O	52301.7750493	kcal mol^{-1} Å^{12}
A_H	−353.3401000	kcal mol^{-1} Å^5
B_H	3467.0790489	kcal mol^{-1} Å^7
C_H	−6549.7630208	kcal mol^{-1} Å^9
D_H	4909.1439175	kcal mol^{-1} Å^{12}
	3-Body Potential Parameters	
F	0.5239824	kcal mol^{-1} Å^{-4}
G	0.1561863	Å^{-1}
H	0.6255337	Å^{-1}

[a] Fixed constant.

by subtracting the SCF energies (E_{Ni} and E_W) of isolated Ni^{2+} and H_2O from that (E_{NiW}) of $[Ni(H_2O)]^{2+}$, as expressed by eq 1.

$$E_{2bd} = E_{NiW} - (E_{Ni} + E_W) \quad (1)$$

To represent the E_{2bd} values by an analytical function, various functions were tested to fit to the E_{2bd} values by a least-squares optimization using the Levenberg−Marquardt algorithm. The best reproducibility was obtained using a function composed of four r^{-m} terms for the non-Coulombic interaction in addition to the Coulombic interaction, as expressed by eq 2,

$$E_{2bd} = \frac{Q_{Ni}Q_O}{r_{NiO}} + A_O r_{NiO}^{-5} + B_O r_{NiO}^{-7} + C_O r_{NiO}^{-9} + D_O r_{NiO}^{-12} + \sum_{i=1}^{2}\left(\frac{Q_{Ni}Q_{Hi}}{r_{NiHi}} + A_H r_{NiHi}^{-5} + B_H r_{NiHi}^{-7} + C_H r_{NiHi}^{-9} + D_H r_{NiHi}^{-12}\right) \quad (2)$$

where Q means the atomic net charge, r_{NiH} is the distance between Ni and H, and A, B, C, and D are optimization parameters. The values of −0.6596 and 0.3298 were adopted for Q_O and Q_H, respectively, from the central-force (CF) model for H_2O.[86] The value of Q_{Ni} was assumed to be 2. E_{2bd} values near the global energy minimum were emphasized during the least-squares procedure by assigning an appropriate weighting factor. E_{2bd} values above 30 kcal mol^{-1} were excluded in the optimization of the function. The optimized potential parameters are given in Table 1 together with constants used in eq 2. The SCF-calculated and fitted E_{2bd} values are plotted in Figure 1 for a variety of θ and ϕ values. The average absolute residual of the fit was 1.3 kcal mol^{-1}. The global energy minimum of the fitted function was found to be −84.4 kcal mol^{-1} at r_{NiO} = 1.95 Å and $\theta = \phi = 0°$.

Evaluation of 3-Body Correction Function. The 3-body correction energy (E_{3bd}) was calculated according to eq 3,

$$E_{3bd} = E_{NiW^iW^j} - (E_{Ni} + 2E_W) - (E_{NiW^i} + E_{NiW^j}) - E_{W^iW^j} \quad (3)$$

where $E_{NiW^iW^j}$ is the SCF energy for $[Ni(H_2O)_2]^{2+}$, E_{NiW^i} and E_{NiW^j} are the 2-body interaction energies, calculated using the previously developed analytical function (eq 2), and $E_{W^iW^j}$ is the intermolecular potential between H_2O molecules computed using the CF2 model.[87] The SCF-energy calculations were performed by varying independently both Ni−O distance ($2.0 \le r_{NiO} \le 6.0$ Å) and the O−Ni−O angle (ψ: $60° \le \psi \le 180°$). The dipole moments of both H_2O molecules were fixed to point toward the Ni(II) ion for all configurations.

Almost all of the E_{3bd} values were found to be positive for the geometries employed in this study. The E_{3bd} value decreases with increasing r_{NiO} and becomes almost 0 kcal mol^{-1} when either r_{NiO} approaches to 6.0 Å. Furthermore, given a set of two r_{NiO} distances, the E_{3bd} value fell off with increasing distance between the two H_2O molecules. The E_{3bd} function can be expressed by eq 4,

$$E_{3bd} = F\exp\{-G(r_{NiO^i} + r_{NiO^j})\} \times \exp(-Hr_{ij})\{(R_{CL} - r_{NiO^i})^2(R_{CL} - r_{NiO^j})^2\} \quad (4)$$

where F, G, and H are fitting parameters, r_{ij} is the distance between two oxygens of H_2O molecules, and R_{CL} is the cutoff limit of 6.0 Å for the 3-body correction function. The final term in eq 4 guarantees that E_{3bd} vanishes if r_{NiO^i} or r_{NiO^j} become larger than R_{CL}. This function is of the same type as used in previous studies.[20,21,88−90] A total of 6205 configurations were generated for SCF-energy calculations of $[Ni(H_2O)_2]^{2+}$. The analytical function of eq 4 was fitted to the E_{3bd} values by a least-squares optimization, and the final parameters are given in Table 1. The average absolute residual of the fit was 1.4 kcal mol^{-1}.

Classical MD Simulation. All classical MD simulations were performed in the *NVT* ensemble with a time step of 0.2 fs using a general predictor-corrector algorithm.[6,7] The density of the simulation box was set to the experimental value of pure water at 298 K (0.997 g cm^{-3}). The periodic boundary condition was applied and the reaction field method was used to treat long-range electrostatic potentials and forces.[6] The temperature of the system was maintained at 298.16 K by the velocity-scaling method with a relaxation time of 100 fs.[91] The CF2 model was used for the intermolecular potential between H_2O molecules,[87] and the intramolecular potential of H_2O developed by Bopp et al. was employed to reproduce correctly liquid-phase vibrational frequencies.[92] Cutoff distances of 3.0 and 5.0 Å were adopted for non-Coulombic interactions between H atoms and between O and H atoms, respectively. All other pair interactions were cut off at 9.0 Å. When 2-body pair potentials and forces were calculated within the spherical cutoff limit, the shifted-force potential technique was used to avoid discontinuity of potential functions at the cutoff limit.[6,7]

The classical MD simulation was performed for a system composed of one Ni(II) ion and 499 H_2O molecules in a simulation box of 15069 Å^3 (24.70 × 24.70 × 24.70 Å). To construct the initial configuration, the O atoms of H_2O were placed in the simulation box according to the face-centered cubic lattice. The H atoms were arranged with random configuration of H_2O molecules. A total of 400 000 steps (80 ps) were first processed using only the 2-body potential. At that time, the system was confirmed to be energetically equilibrated. A further 200 000 steps (40 ps) were sampled to evaluate the structural properties. The classical MD simulation was continued for a further 30 000 000 steps (6.0 ns) after the inclusion of 3-body corrections. All energies were confirmed to become stable within the initial 5 ps.

Classical MC Simulation. All classical MC simulations were performed in the *NVT* ensemble at 298.16 K using the

Metropolis sampling algorithm.[93] The CF2 model was used to describe the intermolecular potentials for H_2O.[92] The system consisted of one Ni(II) ion and 499 H_2O molecules, and the periodic boundary condition was applied. A spherical cutoff with a radius of 12.35 Å (half box length) was adopted for all pair interactions. After a random generation of the initial configuration, 3 000 000 configurations were generated in order to equilibrate the system using only the 2-body potential. An additional 3 000 000 configurations were sampled to measure the structural properties. The 3-body correction function was then included, and 3 000 000 configurations were sampled to evaluate the structural properties after generation of 3 000 000 configurations for the equilibration.

QM/MM-MD Simulation. In the QM/MM-MD simulation, the system composed of the Ni(II) ion and solvent H_2O molecules is separated into the QM and MM regions. As the evaluation of the hydration structure around the Ni(II) ion was the main subject of this study, the Ni(II) ion and its first coordination sphere were selected as the QM region. The remaining H_2O molecules were treated as MM molecules. The effective Hamiltonian $\hat{H}_{\text{eff}}$ for this system is given as

$$\hat{H}_{\text{eff}} = \hat{H}_{\text{QM}} + \hat{H}_{\text{MM}} + \hat{H}_{\text{QM/MM}} \tag{5}$$

where $\hat{H}_{\text{QM}}$ is the Hamiltonian of the Ni(II) ion and its first coordination sphere, $\hat{H}_{\text{MM}}$ is the molecular mechanics Hamiltonian for the interaction between H_2O molecules in the MM region, and $\hat{H}_{\text{QM/MM}}$ is the interaction Hamiltonian between the atoms in the QM region and those in the MM region. The energy of the QM region was determined by SCF calculations at UHF level using the same basis sets as those for the construction of the 2-body potential and the 3-body correction term.[83,84] The forces on the QM atoms were computed by analytic gradients using the Gaussian98 program.[82] The $\hat{H}_{\text{MM}}$ term simply denotes the kinetic and potential energies of H_2O molecules, and the CF2 potential was used to describe the latter.[87,92] The forces acting on MM molecules were computed classically using the molecular mechanical force fields. The coupling Hamiltonian $\hat{H}_{\text{QM/MM}}$ describes the interactions between the QM and MM regions. For this term, the reported 2-body potential function for Ni^{2+} and H_2O with its 3-body correction was applied by embedding of the QM system in the MM molecules.

To guarantee a smooth movement of H_2O molecules between the QM and MM regions, a transition region with a shell thickness of 0.2 Å was introduced by defining two distances, R_{on} and R_{off} ($R_{\text{on}} < R_{\text{off}}$), around the Ni(II) ion. All H_2O molecules at r_{NiO} distances smaller than and equal to R_{on} were treated as part of the QM region, and the forces (F_{QM}) were calculated quantum mechanically. For the molecules with $r_{\text{NiO}} > R_{\text{off}}$, the forces ($F_{\text{MM}}$) were obtained by the first differentiation of the shifted potentials in the same manner as in the classical MD simulation. If the r_{NiO} value was in the range $R_{\text{on}} < r_{\text{NiO}} \leq R_{\text{off}}$, the transition force ($F_{\text{QM}\rightarrow\text{MM}}$) on the atoms was computed according to eq 6,

$$F_{\text{QM}\rightarrow\text{MM}} = S(r_{\text{NiO}})F_{\text{QM}} + (1 - S(r_{\text{NiO}}))F_{\text{MM}} \tag{6}$$

where $S(r_{\text{NiO}})$ is the switching function defined by eq 7.[94]

$$S(r_{\text{NiO}}) = \frac{(R_{\text{off}}^2 - r_{\text{NiO}}^2)^2(R_{\text{off}}^2 + 2r_{\text{NiO}}^2 - 3R_{\text{on}}^2)}{(R_{\text{off}}^2 - R_{\text{on}}^2)^3} \qquad R_{\text{on}} < r_{\text{NiO}} \leq R_{\text{off}} \tag{7}$$

The values of R_{on} and R_{off} were selected to be 3.6 and 3.8 Å,

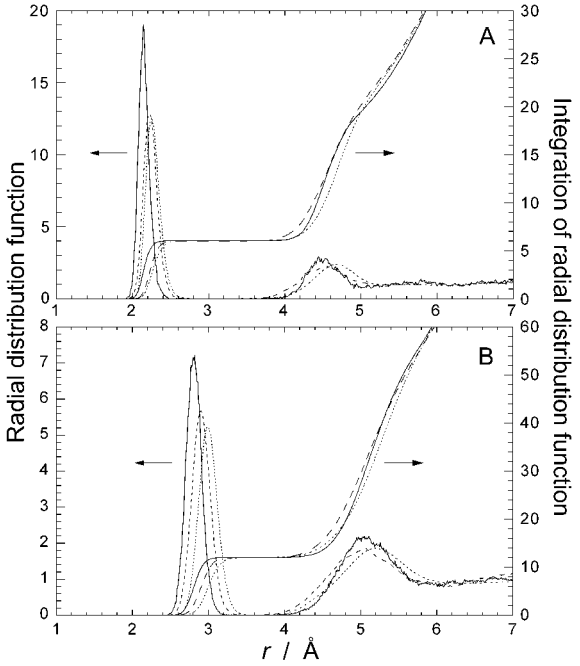

Figure 2. Ni−O (A) and Ni−H (B) radial distribution functions and their running integration numbers. The dotted, broken, and solid lines represent the values obtained by classical MD, classical MC, and QM/MM-MD simulation, respectively.

respectively, according to the radial distribution function (RDF) obtained by the classical MD simulation to include the first coordination sphere of Ni^{2+} in the QM region. The RDF probability of the Ni−O interaction in this transition region was zero during the classical MD simulation (see Figure 2).

The QM/MM-MD simulation was started from an equilibrated configuration taken from a classical MD simulation of one Ni(II) ion in 499 H_2O. The simulation procedure was almost the same as that of the classical MD simulation except for the evaluation of the quantum mechanical forces in the first coordination sphere of the Ni(II) ion. The energetic equilibrium was achieved after 23 000 steps (4.6 ps). A further 35 000 steps (7.0 ps) were processed to measure the structural properties. The QM/MM-MD simulations were performed on a 2CPU SMP Workstation equipped with dual DEC Alpha 21264 processors operating at a clock frequency of 667 MHz. A total of 58 000 ab initio calculations were performed consuming 122.8 days of CPU time.

Results and Discussion

Hydration Structure. To evaluate the hydration structure of the Ni(II) ion, the structural properties obtained by the QM/MM-MD simulation are compared with those of the classical MD and MC simulation using the 3-body correction. Some structure parameters are summarized in Table 2. The RDFs for the Ni−O and Ni−H interactions obtained by the classical and QM/MM simulations are compared in Figure 2. The peaks corresponding to the first and second coordination sphere were clearly separated in all simulations. The maximum probability of Ni−O interaction in the first coordination sphere was observed at 2.25, 2.21, and 2.14 Å for the classical MD, classical MC, and QM/MM-MD simulation, respectively. The difference between the classical MD and MC simulations can be ascribed to the different treatment of the long-range interactions; i.e., the reaction field method was used in the former while no such corrections were adopted in the latter. The average coordination number in the first coordination sphere was 6 according to the

TABLE 2: Hydration Structure Parameters of the Ni(II) Ion in Water Determined by Molecular Simulation Methods

T/K	method[a]	*N*[b]	r_1[c]/Å	n_1[d]	r_2[c]/Å	n_2[d]	ref
		Ni−O Interaction					
298	C-MD	499	2.15	8.0	4.21	28	this work
298	C-MD+3	499	2.25	6.0	4.68	16	this work
298	C-MC	499	2.15	8.0	4.07	21	this work
298	C-MC+3	499	2.21	6.0	4.61	16	this work
298	QM/MM-MD+3	499	2.14	6.0	4.50	13	this work
316	C-MD	64	2.17	8.0	4.2[e]		2
298	C-MC	200	2.09	8.0	4.1[e]	18	3
298	C-MC[f]	200	2.07	6.0	4.2[e]	16	3
298	C-MD	278	2.07	6.0			4
		Ni−H Interaction					
298	C-MD	499	2.87	17.2	4.93	51	this work
298	C-MD+3	499	2.99	12.0	5.18	50	this work
298	C-MC	499	2.76	17.0	4.63	53	this work
298	C-MC+3	499	2.88	12.0	5.06	50	this work
298	QM/MM-MD+3	499	2.81	12.0	5.04	50	this work
316	C-MD	64	2.76		4.7[e]		2
298	C-MC	200	2.75	16.2		44	3
298	C-MC[f]	200	2.69	12.0		38	3

[a] "C-MD", "C-MC", and "QM/MM-MD" correspond to classical MD, classical MC, and QM/MM MD simulation, respectively. "+3" means the inclusion of 3-body corrections. [b] Number of H_2O molecules in the simulation box. [c] r_i is the distance of the *i*th maximum of RDF. [d] n_i is the coordination number obtained by the integration of RDF for the *i*th coordination sphere. [e] Values estimated according to published figures. [f] Polarized water model.

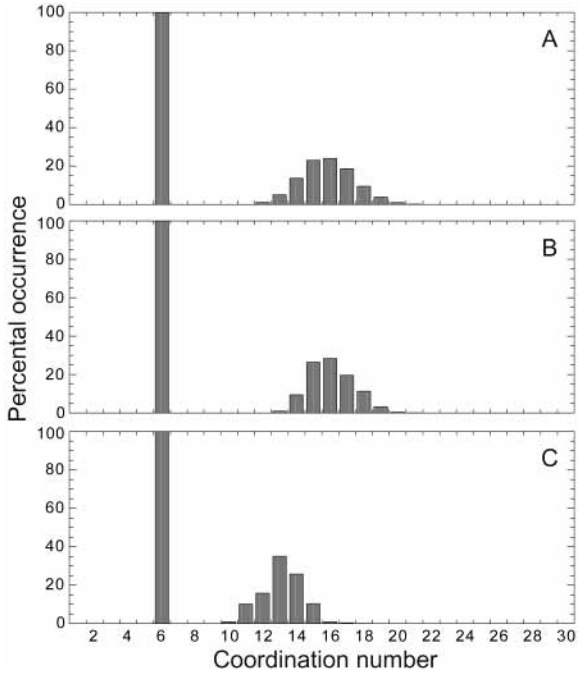

Figure 3. Coordination number probability of first and second hydration sphere of the Ni(II) ion for classical MD (A), classical MC (B), and QM/MM-MD (C) simulation.

running integration number of RDFs for all simulations. The coordination number distribution (CND) probability is shown in Figure 3. In the first coordination sphere, only the coordination number 6 is observed in all simulations. The O−Ni−O angular distribution function (ADF); i.e., the probability to find a certain O−Ni−O angle in the first coordination sphere of the Ni(II) ion, is depicted in Figure 4, in which the integrated function of ADF is included. Because there are six H_2O molecules in the first coordination sphere, the integrated function is scaled to make the overall running integration number 5. It is clearly seen in Figure 4 that there are four nearest-neighboring

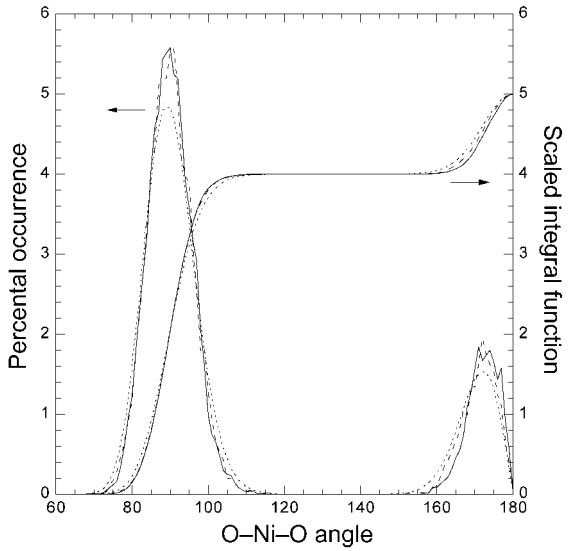

Figure 4. Angular distribution function for the O−Ni−O angle in the first coordination sphere of the Ni(II) ion for classical MD (dotted line), classical MC (broken line), and QM/MM-MD (solid line) simulation. The scaled integrated functions are included.

O atoms at O−Ni−O angles of ca. 90° (89.5°, 90.5°, and 89.1° for the classical MD, classical MC, and QM/MM-MD simulation, respectively) and that there is one other ligand at an O−Ni−O angle of ca. 172° (172.0°, 172.5°, and 172.7° for the classical MD, classical MC, and QM/MM-MD simulation, respectively). According to these data, it is obvious that the hydration geometry around the Ni(II) ion is, on average octahedral, with slight distortions and considerable variability of the O−Ni−O angles (±20°, see Figure 4). The 6-coordinate octahedral hydration structure of the Ni(II) ion is in agreement with the experimental results.

The Ni−O distance (2.14 Å) obtained by the QM/MM-MD simulation cannot be directly compared with the value of 2.06 Å determined experimentally (see Figure S1). The experimental studies using X-ray have been carried out for solutions with high concentration, while a dilute solution is treated in the present simulations. The structure parameters determined experimentally for high concentration solutions must be affected by coexisting counterions. Especially if the counterion locates in the second hydration sphere of the metal ion, the Ni−O distance should be shortened due to the enhanced polarization of coordinating H_2O molecules by the counterion. The choice of basis sets for the QM/MM-MD simulation may also have affected the calculated Ni−O distance. The bond distance certainly depends on the size and quality of basis sets, but the changes are not large, and the present selection was the maximum possible in order to keep computation time within a reasonable limit.

To evaluate the average orientation of H_2O molecules with respect to the Ni(II) ion in the first coordination sphere, an angle (ξ) between the Ni−O vector and the normal vector of the H_2O molecule was defined. According to the trajectory of ξ, it was found that the ξ value was modulated by two phases. The frequencies of these two kinds of oscillational modulation were ca. 2×10^{13} and ca. 2×10^{12} s^{-1}. Although the total simulation period of the QM/MM-MD simulation is much shorter than the classical MD simulation, the sampling for 7.0 ps in the case of the QM/MM-MD simulation is considered to be sufficient to obtain an average value of ξ with appropriate statistics. The angular distribution function of the angle $90 - \xi$ is shown in Figure 5 for the classical and QM/MM-MD simulations. The

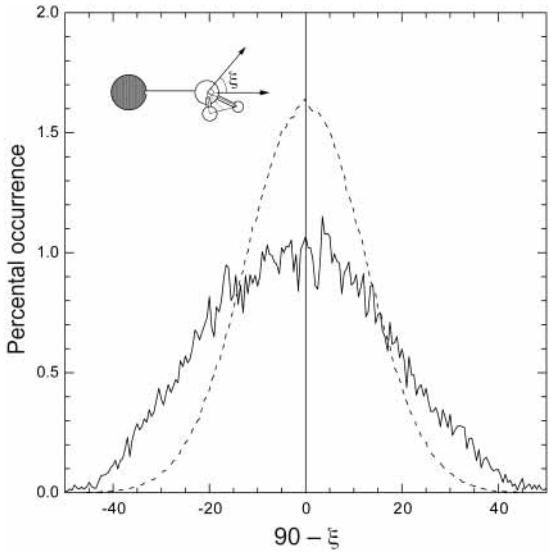

Figure 5. Angular distribution function for the angle $90 - \xi$ (definition see text) in the first coordination sphere of the Ni(II) ion for the classical MD (dotted line) and QM/MM-MD (solid line) simulation.

maximum probability of $90 - \xi$ is observed at ca. 0° for both simulations. The values of $90 - \xi$ for the QM/MM-MD simulation are, however, more broadly distributed in comparison with those of the classical MD simulation. The occurrence probability is nearly constant in the range from −15° to +15° in the case of the QM/MM-MD simulation; hence the inclusion of electronic contributions increases the probability of tilted arrangements of the H_2O molecules in the first coordination sphere.

As seen in Figure 2, the second peak corresponding to H_2O molecules in the second hydration sphere for the QM/MM-MD simulation shifts to a shorter distance and becomes narrower in comparison with classical simulations. Furthermore, according to Figure 3, the maximum probability of CND in the second hydration sphere is observed at a smaller number for the QM/MM-MD simulation compared with classical simulations; i.e., the CND probability is in the range from 11 to 15 with the maximum at 13 for the former and from 13 to 19 with the maximum at 16 for the latter. The hydration number of 13 for the QM/MM-MD simulation indicates that H_2O molecules in the second hydration sphere arrange almost ideally to form hydrogen bonds with the H_2O ligands in the first hydration sphere. On the other hand, the value of 16 in the classical simulations means that some additional H_2O molecules interacting without such a specific arrangement are included in the second hydration sphere in addition to the hydrogen-bonded ones. The exclusion of these additional H_2O molecules from the second hydration sphere reduces intermolecular repulsions between H_2O molecules, and the shorter $Ni-O^{II}$ (second shell) distance in the QM/MM-MD simulation thus reflects the decreased hydration number. A similar conclusion has been reported in a previous QM/MM-MC simulation of the hydrated Cu(II) ion.[64] The quantum mechanical treatment of the first hydration sphere significantly affects the structure of the second hydration sphere as well, indicating a spillover effect of approximations in the first coordination sphere to regions located farther away.

Effect of the 3-Body Correction. The effect of the 3-body correction function was examined within the framework of the classical MD and MC simulations. The results are summarized in Figure S2, in which the RDFs for the Ni−O atomic pair, the ADFs, and the CNDs are shown for the classical simulations with and without 3-body corrections. The structure parameters are given in Table 2. As is clearly seen in Figure S2, an 8-coordinate hydration structure is predominant in simulations without 3-body corrections. On the other hand, the 6-coordinate hydration structure is observed with 100% probability after inclusion of 3-body corrections in both classical MD and MC simulations. This means that the simulation using only the developed 2-body potential is unable to obtain the correct hydration structure. A similar decrease in the coordination number has been observed in previous studies for other metal ions using the same or similar type of 3-body correction function.[42−44,95−97] Thus it is evident that additivity of the 2-body potential constructed by ab initio molecular orbital calculations is invalid also in the case of the Ni(II) ion.

It has been experimentally observed and predicted by quantum chemical calculations that a reduced coordination number causes a shortening of the distance between the metal ion and the coordinating atom.[98−100] In the present molecular simulation, however, the Ni−O distance is elongated by the inclusion of the 3-body correction function, although the coordination number is reduced from 8 to 6. Because interligand repulsions around the Ni(II) ion are decreased by the lower coordination number, the longer Ni−O distance observed in classical MD and MC simulations after inclusion of 3-body corrections should be an artifact of both 2-body and 3-body correction functions used in this study or an indication of the importance of higher-order correction terms. (It is known that *n*-body corrections can have alternating signs leading to convergence only after inclusion of more than 3-body terms.) The Ni−O distance in the first coordination sphere obtained by the QM/MM-MD simulation is clearly shorter than the corresponding values of the classical simulations, which can be seen as an indication in that sense. Furthermore, it has been reported that the repulsive E_{3bd} value has a maximum at short M−O distances.[21−23] A proper inclusion of this effect in the 3-body correction function may thus improve the Ni−O distance in the first coordination sphere in classical simulations.

The 3-body corrections play an important role for the structure of the second coordination sphere as well as the first coordination sphere in classical simulations. In the case of the QM/MM-MD simulation, the 3-body corrections are still effective for H_2O molecules in the second hydration sphere of Ni^{2+}. It is known that the 3-body correction term becomes negative when a bound H_2O molecule interacts with another H_2O molecule through a hydrogen bond.[21−26,46] The negative E_{3bd} value is interpreted in terms of the polarization effect of the bound H_2O molecule. An additional consideration of such attractive interactions in the formulation of the 3-body correction function may also contribute to shorten the distance from Ni^{2+} to oxygens in the second hydration sphere.

Water Exchange Reaction. In this study, the classical MD simulation including 3-body corrections was started from an equilibrated configuration of the corresponding simulation without 3-body corrections, in which the Ni(II) ion was surrounded by eight H_2O molecules. During the equilibration, the coordination number of the Ni(II) ion decreased from 8 to 6, and the 6-coordinate structure appeared first about 13 ps after the inclusion of 3-body corrections. During this equilibration period for 13 ps, the total energy of the system relaxed from −2907 kcal mol^{-1} (initial) to −3023 kcal mol^{-1} (average value for 14−18 ps), which is almost comparable to the average energy (−3046 kcal mol^{-1}) with the modulation of ca. ±50 kcal mol^{-1} of the fully equilibrated system (1−6 ns). This indicates that the system was almost equilibrated before the

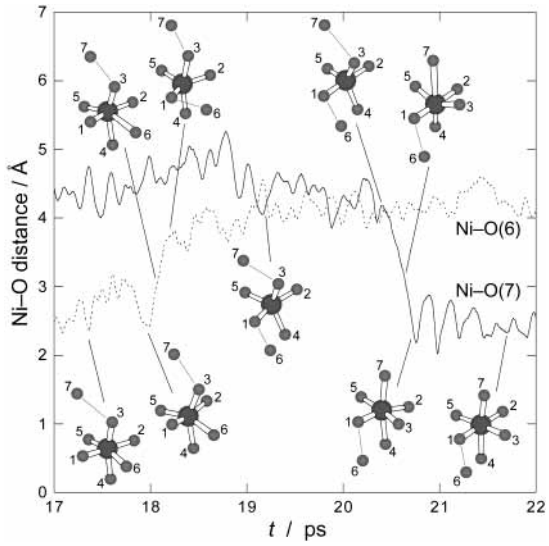

Figure 6. Bond distance trajectories for Ni−O pairs participating in the water exchange reaction calculated by classical MD simulation.

water exchange reaction observed. Subsequently, one H_2O molecule dissociated from $[Ni(H_2O)_6]^{2+}$ at about 18 ps, and another H_2O molecule entered the first coordination sphere at about 20.5 ps of simulation time. The total potential energy between Ni^{2+} and the O atoms shows an energy barrier of ca. 50 kcal mol^{-1} during this water exchange reaction, as shown in Figure S3. After this water exchange reaction, the six H_2O molecules surrounding the Ni(II) ion always stayed in the first coordination sphere up to the final simulation time of 6.0 ns.

The Ni−O distance trajectories of the two H_2O molecules involved in the water exchange reaction are depicted in Figure 6, in which also some instantaneous geometries for the seven O atoms of the ligands around the Ni(II) ion are included. As can be clearly seen from this figure, the water exchange reaction proceeds via a dissociative mode of activation; i.e., one of six H_2O molecules (refer to O(6), Figure 6) first dissociates to form a 5-coordinate intermediate, and then another H_2O molecule (O(7)) enters into the first coordination sphere. This observation is consistent with the dissociative nature for ligand exchange and substitution reactions of the Ni(II) ion demonstrated experimentally[68−71] and theoretically.[76−78]

According to Figure 6, the water exchange reaction is initially induced by a structural distortion of the first coordination sphere, which may be promoted by a repulsive interaction between O(3) and the approaching O(7). The leaving O(6) molecule then starts to dissociate from the Ni(II) ion due to the repulsion between O(6) and O(3), and the dissociation is facilitated by the formation of an intermediate hydrogen bond between O(6) and O(1). The formation of the 5-coordinate intermediate is completed by the entry of O(6) into the second hydration sphere. The configuration of the other H_2O molecules (O(1)−O(5)) remains rather constant during the dissociation process, and thus the five H_2O molecules form a square pyramidal configuration with O(5) as the apex. The 5-coordinate intermediate has a lifetime of ca. 2.5 ps. During this interval, the apex of the pyramid changes from O(5) to O(4), which will occupy the trans position to the entering O(7) after the completion of the water exchange. The configurational change in the intermediate proceeds via an approximately trigonal-bipyramidal configuration with the equatorial plane composed of O(3), O(4), and O(5). The geometrical rearrangement allows O(7) to enter the first coordination sphere, and then the O(7) molecule binds regularly to the Ni(II) ion, forming $[Ni(H_2O)_6]^{2+}$ again.

It should be mentioned that such a detailed picture of the water exchange reaction has not yet been obtained by the most reliable QM/MM-MD simulation, but so far only by the classical MD simulation including 3-body corrections. The present molecular motions around the Ni(II) ion are, however, considered to be a model of the ligand exchange reaction when the reaction proceeds via the dissociative mode of activation. Although the observation of several water exchange reactions would be necessary to discuss the exchange rate, it has to be expected that the interval between the water exchange processes at the Ni(II) ion is on the order of milliseconds according to the experimental rate constant.[70] Such long simulations to observe several water exchange reactions are still far beyond the present computational resources, even for classical MD simulations.

Conclusion

A 6-coordinate hydration structure is observed in QM/MM-MD simulation, and the average structure parameters are in good agreement with the experimental values. The 6-coordinate hydration structure is also observed in classical MD and MC simulations with 3-body corrections, and it is clearly indicated that the inclusion of 3-body corrections is necessary in classical simulations to reproduce the correct coordination number of the first coordination sphere of Ni^{2+}. However, in more detail, the present classical potential functions may not be sufficient to describe correctly the Ni−O distance in the first coordination sphere, because the distance (2.14 Å) obtained by the QM/MM-MD simulation, which includes the many-body effects higher than 3-body, is significantly shorter than the corresponding distances (2.21−2.25 Å) in classical simulations. This clearly means that higher-order corrections are important to obtain a correct Ni−O distance. The reproducibility of the Ni−O distance in classical simulations may be improved by including the relaxation effect of exchange repulsions into the 3-body correction function. Furthermore, the difference in RDF and CND between the classical and QM/MM simulations indicates that a more diffuse arrangement of H_2O molecules in the second hydration sphere is favored by classical simulations. The additional consideration of secondary ($H_2O^{I}-H_2O^{II}$) polarization effects in the 3-body correction function would strengthen the hydrogen-bonding interaction between H_2O molecules in the first and second hydration sphere, thus leading to a more rigid and compact second hydration sphere in classical simulations.

The MD simulation proved a very powerful tool to observe the ligand exchange reaction at metal ions. A detailed picture of the exchange process can be obtained by the MD simulation, although the limitation of computational resources still prevents the observation of several exchange reactions as well as the application of the most sophisticated QM/MM-MD simulation technique for this purpose. For the water exchange reaction of the Ni(II) ion, the dissociative mechanism observed in the classical MD simulation supports the mechanistic hypotheses based on experimental results. The lifetime of the 5-coordinate intermediate, which is difficult to determine experimentally, can be well estimated to be ca. 2.5 ps.

Acknowledgment. This work was partly supported by Grant-in-Aid for Scientific Research (No. 11554030) from the Ministry of Education, Science, Sports, and Culture of Japan, and by a grant of the Austrian Science Foundation (FWF Project No. P13644-TPH). A grant of the Austrian Federal Ministry for Foreign Affairs for A.M.M. is gratefully acknowledged.

Supporting Information Available: The hydration structure parameters determined using the XRD, ND, and EXAFS

techniques in aqueous solution (Table S1), the Ni−O bond distances of $[Ni(H_2O)_6]^{2+}$ in single crystals (Table S2), the Ni−O bond distance distribution probability in aqueous solutions and single crystals (Figure S1), the RDF for the Ni−O atomic pair, the ADF, and the CND obtained by classical MD and MC simulations (Figure S2), the total potential energy between Ni^{2+} and O atoms during the water exchange reaction (Figure S3). This material is available free of charge via the Internet at http://pubs.acs.org.

References and Notes

(1) Ohtaki, H.; Radnai, T. *Chem. Rev.* **1993**, *93*, 1157.
(2) Bounds, D. G. *Mol. Phys.* **1985**, *54*, 1335.
(3) Cordeiro, M. N. D. S.; Ignaczak, A.; Gomes, A. N. F. *Chem. Phys.* **1993**, *176*, 97.
(4) Wallen, S. L.; Palmer, B. J.; Fulton, J. L. *J. Chem. Phys.* **1998**, *108*, 4039.
(5) Hoffmann, M. M.; Darab, J. G.; Palmer, B. J.; Fulton, J. L. *J. Phys. Chem. A* **1999**, *103*, 8471.
(6) Allen, M. P.; Tildesley, D. J. *Computer Simulation of Liquids*; Clarendon Press: Oxford, U.K., 1987.
(7) Haile, J. M. *Molecular Dynamics Simulation*; John Wiley & Sons: New York, 1992.
(8) Clementi, E.; Barsotti, R. *Chem. Phys. Lett.* **1978**, *59*, 21.
(9) Heinzinger, K. *Pure Appl. Chem.* **1985**, *57*, 1031.
(10) Nguyen, H. L.; Adelman, S. A. *J. Chem. Phys.* **1984**, *81*, 4564.
(11) Jancsó, G.; Heinzinger, K.; Bopp, P. *Z. Naturforsch.* **1985**, *40A*, 1235.
(12) Periole, X.; Allouche, D.; Daudey, J.-P.; Sanejouand, Y.-H. *J. Phys. Chem. B* **1997**, *101*, 5018.
(13) Kollman, P. A.; Kuntz, I. D. *J. Am. Chem. Soc.* **1972**, *94*, 9236.
(14) Probst, M. M. *Chem. Phys. Lett.* **1987**, *137*, 229.
(15) Caldwell, J.; Dang, L. X.; Kollman, P. A. *J. Am. Chem. Soc.* **1990**, *112*, 9144.
(16) Bock, C. W.; Katz, A. K.; Glusker, J. P. *J. Am. Chem. Soc.* **1995**, *117*, 3754.
(17) Tsutsui, Y.; Sugimoto, K.; Wasada, H.; Inada, Y.; Funahashi, S. *J. Phys. Chem. A* **1997**, *101*, 2900.
(18) Pavlov, M.; Siegbahn, P. E. M.; Sandström, M. *J. Phys. Chem. A* **1998**, *102*, 219.
(19) Lubin, M. I.; Bylaska, E. J.; Weare, J. H. *Chem. Phys. Lett.* **2000**, *322*, 447.
(20) Lybrand, T. P.; Kollman, P. A. *J. Chem. Phys.* **1985**, *83*, 2923.
(21) Clementi, E.; Kistenmacher, H.; Kolos, W.; Romano, S. *Theor. Chim. Acta* **1980**, *55*, 257.
(22) Ortega-Blake, I.; Novaro, O.; Les, A.; Rybak, S. *J. Chem. Phys.* **1982**, *76*, 5405.
(23) Ortega-Blake, I.; Hernández, J.; Novaro, O. *J. Chem. Phys.* **1984**, *81*, 1894.
(24) Kollman, P. *J. Am. Chem. Soc.* **1977**, *99*, 4875.
(25) Elrod, M. J.; Saykally, R. J. *Chem. Rev.* **1994**, *94*, 1975.
(26) Kistenmacher, H.; Popkie, H.; Clementi, E. *J. Chem. Phys.* **1974**, *61*, 799.
(27) Mezei, M.; Beveridge, D. L. *J. Chem. Phys.* **1981**, *74*, 6902.
(28) Impey, R. W.; Madden, P. A.; McDonald, I. R. *J. Phys. Chem.* **1983**, *87*, 5071.
(29) Bopp, P.; Okada, I.; Ohtaki, H.; Heinzinger, K. *Z. Naturforsch.* **1985**, *40a*, 116.
(30) Yamaguchi, T.; Ohtaki, H.; Spohr, E.; Pálinkás, G.; Heinzinger, K.; Probst, M. M. *Z. Naturforsch.* **1986**, *41a*, 1175.
(31) Pálinkás, G.; Heinzinger, K. *Chem. Phys. Lett.* **1986**, *126*, 251.
(32) González-Lafont, A.; Lluch, J. M.; Oliva, A.; Bertrán, J. *Chem. Phys.* **1987**, *111*, 241.
(33) Curtiss, L. A.; Halley, J. W.; Hautman, J.; Rahman, A. *J. Chem. Phys.* **1987**, *86*, 2319.
(34) Meier, W.; Bopp, P.; Probst, M. M.; Spohr, E.; Lin, J.-I. *J. Phys. Chem.* **1990**, *94*, 4672.
(35) Floris, F. M.; Persico, M.; Tani, A.; Tomasi, J. *Chem. Phys. Lett.* **1994**, *227*, 126.
(36) Floris, F.; Persico, M.; Tani, A.; Tomasi, J. *Chem. Phys. Lett.* **1992**, *199*, 518.
(37) Cordeiro, M. N. D. S.; Gomes, J. A. N. F. *J. Comput. Chem.* **1993**, *14*, 629.
(38) Rustad, J. R.; Hay, B. P.; Halley, J. W. *J. Chem. Phys.* **1995**, *102*, 427.
(39) Bernal-Uruchurtu, M. I.; Ortega-Blake, I. *J. Chem. Phys.* **1995**, *103*, 1588.
(40) Kowall, T.; Foglia, F.; Helm, L.; Merbach, A. E. *J. Am. Chem. Soc.* **1995**, *117*, 3790.
(41) Cieplak, P.; Kollman, P. *J. Chem. Phys.* **1990**, *92*, 6761.
(42) Probst, M. M.; Spohr, E.; Heinzinger, K.; Bopp, P. *Mol. Simul.* **1991**, *7*, 43.
(43) Texler, N. R.; Rode, B. M. *J. Phys. Chem.* **1995**, *99*, 15714.
(44) Marini, G. W.; Texler, N. R.; Rode, B. M. *J. Phys. Chem.* **1996**, *100*, 6808.
(45) Curtiss, L. A.; Halley, J. W.; Hautman, J. *Chem. Phys.* **1989**, *133*, 89.
(46) Curtiss, L. A.; Jurgens, R. *J. Phys. Chem.* **1990**, *94*, 5509.
(47) Warshel, A.; Levitt, M. *J. Mol. Biol.* **1976**, *103*, 227.
(48) Field, M. J.; Bash, P. A.; Karplus, M. *J. Comput. Chem.* **1990**, *11*, 700.
(49) Åqvist, J.; Warshel, A. *Chem. Rev.* **1993**, *93*, 2523.
(50) Gao, J. In *Reviews in Computational Chemistry*; Lipkowitz, K. B., Boyd, D. B., Eds.; VCH: New York, 1996; Vol. 7.
(51) Bakowies, D.; Thiel, W. *J. Phys. Chem.* **1996**, *100*, 10580.
(52) Mordasini, T. Z.; Thiel, W. *Chimia* **1998**, *52*, 288.
(53) Gao, J. *J. Am. Chem. Soc.* **1993**, *115*, 2930.
(54) Sehgal, A.; Shao, L.; Gao, J. *J. Am. Chem. Soc.* **1995**, *117*, 11337.
(55) Gao, J.; Li, N.; Freindorf, M. *J. Am. Chem. Soc.* **1996**, *118*, 4912.
(56) Lyne, P. D.; Mulholland, A. J.; Richards, W. G. *J. Am. Chem. Soc.* **1995**, *117*, 11345.
(57) Bryce, R. A.; Vincent, M. A.; Hillier, I. H. *J. Phys. Chem. A* **1999**, *103*, 4094.
(58) Svanberg, M.; Pettersson, J. B. C.; Bolton, K. *J. Phys. Chem. A* **2000**, *104*, 5787.
(59) Kerdcharoen, T.; Liedl, K. R.; Rode, B. M. *Chem. Phys.* **1996**, *211*, 313.
(60) Tongraar, A.; Liedl, K. R.; Rode, B. M. *J. Phys. Chem. A* **1997**, *101*, 6299.
(61) Tongraar, A.; Liedl, K. R.; Rode, B. M. *Chem. Phys. Lett.* **1998**, *286*, 56.
(62) Tongraar, A.; Liedl, K. R.; Rode, B. M. *J. Phys. Chem. A* **1998**, *102*, 10340.
(63) Tongraar, A.; Rode, B. M. *J. Phys. Chem. A* **1999**, *103*, 8524.
(64) Marini, G. W.; Liedl, K. R.; Rode, B. M. *J. Phys. Chem. A* **1999**, *103*, 11387.
(65) Kerdcharoen, T.; Rode, B. M. *J. Phys. Chem. A* **2000**, *104*, 7073.
(66) Yagüe, J. I.; Mohammed, A. M.; Loeffler, H.; Rode, B. M. *J. Phys. Chem. A* **2001**, *105*, 7646.
(67) Schwenk, C. F.; Loeffler, H. H.; Rode, B. M. *J. Chem. Phys.* **2001**, *115*, 10808.
(68) Wilkins, R. G. *The Study of Kinetics and Mechanism of Reactions of Transition Metal Complexes*; Allyn and Bacon: Boston, 1974.
(69) Margerum, D. W.; Cayley, G. R.; Weatherburn, D. C.; Pagenkopf, G. K. In *Coordination Chemistry*; Martell, A. E., Ed.; ACS Monograph 174; American Chemical Society: Washington, DC, 1978.
(70) Lincoln, S. F.; Merbach, A. E. *Adv. Inorg. Chem.* **1995**, *42*, 1.
(71) Wilkins, R. G. *Comments Inorg. Chem.* **1983**, *2*, 187.
(72) Wilkins, R. G.; Eigen, M. *Adv. Chem. Ser.* **1965**, *49*, 55.
(73) Fuoss, R. M. *J. Am. Chem. Soc.* **1958**, *80*, 5059.
(74) Langford, C. H.; Gray, H. B. *Ligand Substitution Processes*; Benjamin: New York, 1966.
(75) Meyer, F. K.; Newman, K. E.; Merbach, A. E. *J. Am. Chem. Soc.* **1979**, *101*, 5588.
(76) Rotzinger, F. P. *J. Am. Chem. Soc.* **1996**, *118*, 6760.
(77) Rotzinger, F. P. *J. Am. Chem. Soc.* **1997**, *119*, 5230.
(78) Tsutsui, Y.; Wasada, H.; Funahashi, S. *Bull. Chem. Soc. Jpn.* **1998**, *71*, 1771.
(79) Rey, R.; Hynes, J. T. *J. Phys. Chem.* **1996**, *100*, 5611.
(80) Spångberg, D.; Wojcik, M.; Hermansson, K. *Chem. Phys. Lett.* **1997**, *276*, 114.
(81) Hermansson, K.; Wojcik, M. *J. Phys. Chem. B* **1998**, *102*, 6089.
(82) Frisch, M. J.; Trucks, G. W.; Schlegel, H. B.; Scuseria, G. E.; Robb, M. A.; Cheeseman, J. R.; Zakrewski, V. G.; Montgomery, J. A.; Stratmann, R. E.; Burant, J. C.; Dapprich, S.; Millam, J. M.; Daniels, A. D.; Kudin, K. N.; Strain, M. C.; Farkas, O.; Tomasi, J.; Barone, V.; Cossi, M.; Cammi, R.; Mennucci, B.; Pomelli, C.; Adamo, C.; Clifford, S.; Ochterski, J.; Petersson, G. A.; Ayala, P. Y.; Cui, Q.; Morokuma, K.; Malick, D. K.; Rabuck, A. D.; Raghavachari, K.; Foresman, J. B.; Cioslowski, J.; Ortiz, J. V.; Stefanov, B. B.; Liu, G.; Liashenko, A.; Piskorz, P.; Komaromi, I.; Gomperts, R.; Martin, R. L.; Fox, D. J.; Keith, T.; Al-Laham, M. A.; Peng, C. Y.; Nanayakkara, A.; Gonzalez, C.; Challacombe, M.; Gill, P. M. W.; Johnson, B. G.; Chen, W.; Wong, M. W.; Andres, J. L.; Head-Gordon, M.; Replogle, E. S.; Pople, J. A. *Gaussian 98*, Revision A.7; Gaussian, Inc.: Pittsburgh, PA, 1998.
(83) Hay, P. J.; Wadt, W. R. *J. Chem. Phys.* **1985**, *82*, 299.
(84) Dunning, T. H., Jr.; Hay, P. J. In *Modern Theoretical Chemistry*; Schaefer, H. F., III, Ed.; Plenum Press: New York, 1976; Vol. 3.
(85) Kuchitsu, K.; Morino, Y. *Bull. Chem. Soc. Jpn.* **1965**, *38*, 814.
(86) Lemberg, H. L.; Stillinger, F. H. *J. Chem. Phys.* **1975**, *62*, 1677.
(87) Stillinger, F. H.; Rahman, A. *J. Chem. Phys.* **1978**, *68*, 666.
(88) Dang, L. X.; Rice, J. E.; Caldwell, J.; Kollman, P. A. *J. Am. Chem. Soc.* **1991**, *113*, 2481.

(89) Perera, L.; Berkowitz, M. L. *J. Chem. Phys.* **1991**, *95*, 1954.
(90) Dang, L. X. *J. Chem. Phys.* **1992**, *96*, 6970.
(91) Berendsen, H. J. C.; Postma, J. P. M.; van Gunsteren, W. F.; DiNola, A.; Haak, J. R. *J. Chem. Phys.* **1984**, *81*, 3684.
(92) Bopp, P.; Jancsó, G.; Heinzinger, K. *Chem. Phys. Lett.* **1983**, *98*, 129.
(93) Metropolis, N.; Rosenbluth, A. W.; Rosenbluth, M. N.; Teller, A. H.; Teller, E. *J. Chem. Phys.* **1953**, *21*, 1087.
(94) Brooks, B. R.; Bruccoleri, R. E.; Olafson, B. D.; States, D. J.; Swaminathan, S.; Karplus, M. *J. Comput. Chem.* **1983**, *4*, 187.
(95) Hannongbua, S. *J. Chem. Phys.* **1997**, *106*, 6076.
(96) Sidhisoradej, W.; Hannongbua, S.; Ruffolo, D. *Z. Naturforsch.* **1998**, *53a*, 208.
(97) Pranowo, H. D.; Rode, B. M. *J. Phys. Chem. A* **1999**, *103*, 4298.
(98) Inada, Y.; Sugimoto, K.; Ozutsumi, K.; Funahashi, S. *Inorg. Chem.* **1994**, *33*, 1875.
(99) Ozutsumi, K.; Abe, Y.; Takahashi, R.; Ishiguro, S. *J. Phys. Chem.* **1994**, *98*, 9894.
(100) Funahashi, S.; Inada, Y. *Trends Inorg. Chem.* **1998**, *5*, 15.